Molecular orientation arrangements in the smectic-*C** variant liquid-crystal phases

D. A. Olson, X. F. Han, A. Cady, and C. C. Huang
School of Physics and Astronomy, University of Minnesota, Minneapolis, Minnesota 55455
(Received 30 October 2001; revised manuscript received 20 May 2002; published 6 August 2002)

Recent experiments have identified three-layer and four-layer distorted helical structures in the smectic liquid-crystal phases Sm C^*_{FI1} and Sm C^*_{FI2}, respectively. However, no theories have explained the existence of all these phases. A discrete phenomenological model of the free-energy is analyzed and found to predict the stability of distorted three-layer and four-layer structures, as well as simple helical solutions in smectic liquid crystals. A simple physical picture is provided to explain the stability of the phases exhibiting distorted helical structures.

DOI: 10.1103/PhysRevE.66.021702 PACS number(s): 61.30.Cz

I. INTRODUCTION

Understanding ordering is a principal goal of physics. The competition between different interactions manifests in the existence of various phases of condensed matter systems. In this paper we examine an orientational ordering observed in liquid crystals arising from a competition between interlayer interactions. This ordering is seen in some smectics, which are layered liquid-crystal phases with no long-range positional ordering within each layer. In the smectic-*C* (Sm-*C*) phase the molecular long axes are tilted from the layer normal. In the attempt to synthesize compounds exhibiting the chiral Sm-*C* (Sm-*C**) phase with a large spontaneous polarization, different phases were discovered. The only apparent difference between these phases is the progression of the molecular orientation from layer to layer. First the antiferroelectric Sm-*C** (Sm-C^*_{A}) phase was discovered, thereby demonstrating that antiferroelectric ordering can exist without long-range positional ordering [1,2]. Subsequently, the antiferroelectric phase with a four-layer unit cell (Sm C^*_{FI2}), the ferrielectric phase with a three-layer unit cell (Sm C^*_{FI1}), and the optically uniaxial phase (Sm C^*_{α}) were identified. Some of these have been used in high-speed electro-optical switches [3]. Experiments support distorted helical structures for the Sm-C^*_{FI2} and Sm-C^*_{FI1} phases, and an incommensurate short-pitched helix for the Sm-C^*_{α} phase with a pitch length of greater than four layers [4–6]. The Sm-C^*_{α} phase arises from competition between nearest-neighbor and next-nearest-neighbor interactions [7,8]. No simple and complete explanation for the existence of the Sm-C^*_{FI2} and Sm-C^*_{FI1} phases is available, although attempts have been made [9–11]. We present a discrete phenomenological model that predicts distorted four-layer (Sm-C^*_{d4}) and three-layer (Sm-C^*_{d3}) phases, which may describe the Sm-C^*_{FI2} and Sm-C^*_{FI1} phases, respectively. Moreover, two distinct Sm-C^*_{α} phases with different pitch size separated by the Sm-C^*_{d4} phase are found. In addition, the model yields the molecular arrangements for the Sm-*C** and Sm-C^*_{A} phases.

In what follows we first present a discrete phenomenological model and discuss the six phases that it predicts. We next discuss the phase diagram that results from the model. A simplified version of the free-energy is then presented, which contains all of the components necessary to give a complete phase diagram in order to guide future theoretical work. A thorough discussion of the results follows.

II. MODEL

To construct a phenomenological model of the Sm-*C** variant phases we need to define the vector $\vec{\xi}_j = \theta[\cos(\alpha_j),\sin(\alpha_j)]$ that describes the molecular tilt in layer j. θ and α_j are the tilt magnitude and azimuthal orientation, respectively. Figure 1(a) shows a cartoon of a single smectic layer while the ellipsoid in Fig. 1(b) represents the average molecular orientation of this layer. θ and α for this layer are also shown. α is defined as the angle between an arbitrarily chosen vector in the layer plane (in the picture the vector is $\hat{x}$) and the vector oriented along the projection of the molecule onto the layer plane. θ is the angle between the layer normal direction ($\hat{z}$) and the molecular long axis.

It is known that the direct interactions beyond the nearest neighbors are small due to the lack of positional correlations between molecules in distant layers [12]. However, Čepič and Žekš have considered both polar and tilt ordering and shown that effective interactions up to fourth-nearest neighbor can be significant [13]. For the steric interactions described below a term proportional to $(\vec{\xi}_j \cdot \vec{\xi}_{j+1})^2$ is included in the free-energy (G). We write G of a sample with N layers as

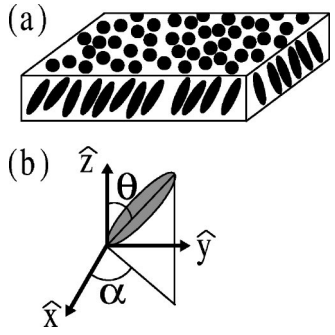

FIG. 1. (a) A cartoon of one smectic layer. (b) A cartoon displaying the average molecular orientation and the angles θ and α. More detail is given in the text.

$$G = A\sum_{j=1}^{N}\left(\frac{T-T_0}{2}\vec{\xi}_j^{\,2} + \frac{B}{4}\vec{\xi}_j^{\,4} + \sum_{i=1}^{3} f_i(\vec{\xi}_j \times \vec{\xi}_{j+i})_z + \sum_{i=1}^{4} a_i(\vec{\xi}_j \cdot \vec{\xi}_{j+i}) + b(\vec{\xi}_j \cdot \vec{\xi}_{j+1})^2\right). \quad (1)$$

Here T_0 is the ''unrenormalized'' transition temperature to the tilted phases. The first two terms are the usual mean-field expansion of the free-energy in terms of the primary order parameter. The three f_i terms describe effective interlayer chiral interactions up to third-nearest neighbors and the four a_i terms account for effective interlayer interactions up to fourth-nearest neighbors that are not chiral in nature. A plausible physical origin of these expansion parameters, a_i and f_i, can be found elsewhere [13,14]. This free-energy with $b>0$ and no terms beyond next-nearest neighbors was previously considered. It was suggested that b arose from interactions between quadrupolarly ordered transverse molecular dipoles in neighboring layers and should be positive [7]. Here we argue that steric interactions are significant and prefer a change in α in adjacent layers of 0 or π over $\pi/2$, and make $b<0$. The compounds exhibiting these phases typically have a hockey stick shape [15]. This is probably the cause of these steric interactions. For $b>0$ only Sm C^*, Sm C_A^*, Sm C_α^*, and the bilayer phase (Sm C_{Bi}^*) are stable solutions of the free-energy. However, $b<0$ suppresses Sm C_{Bi}^* and stabilizes Sm C_{d3}^* and Sm C_{d4}^*. According to the analysis by Čepič and Žekš, the effective interactions typically follow $|a_1|>|a_2|>|a_3|>|a_4|$ and $|f_1|>|f_2|>|f_3|$, although this rule does not need to be strictly followed [13]. The parameter a_3 should be negative, while the other terms may be of either sign.

To find a minimum of G numerically, only terms depending on α_j explicitly were considered. With a fixed set of parameters, we set α_j for each layer of our simulated film (typically 30–100 layers in thickness) to a random value between 0 and 2π. The layers were rotated until a local minimum was found. To find the global minimum, this procedure was repeated from 10 to 100 times. To calculate the phase diagrams and physical quantities, such as the pitch, more quickly, we also input trial structures and found the parameters and structure that gave the lowest free-energy. Points along such curves were checked with the first technique to be certain that the structure with the global minimum free-energy was found.

III. DISCUSSION

Figure 2 displays the tilt orientation projected onto the layer plane (c director) for phases that minimize G. Figure 2(a) depicts the c director for the Sm-C^* phase; the α vector for this phase is $(0,\phi,2\phi,3\phi,\ldots)$. Given a layer spacing (d), the length of the helical pitch is $d^*2\pi/\phi$. The same α vector can be written for the Sm-C_A^* [Fig. 2(b)], Sm-$C_{\alpha 1}^*$ [Fig. 2(c)], and Sm-$C_{\alpha 2}^*$ [Fig. 2(d)] phases. If $\phi \approx \pi$ then the phase is denoted as Sm C_A^*; if $|\phi|<\pi/2$ or $|\phi|>\pi/2$ we call it Sm $C_{\alpha 1}^*$ or Sm $C_{\alpha 2}^*$, respectively. In the parameter space we have studied, the two Sm-C_α^* phases are separated by the Sm-C_{d4}^* phase. Figures 2(e) and 2(f) depict the c director for the Sm-C_{d4}^* and Sm-C_{d3}^* phases, respectively. The α vectors for Sm C_{d4}^* and Sm C_{d3}^* are $(0,\delta,\pi+2\phi,\pi+2\phi+\delta,4\phi,\ldots)$ and $(0,\pi-\delta/2+\phi,\pi+\delta/2+2\phi,3\phi,\ldots)$, respectively. The distortion angles from the undistorted helical structure with four- and three-layer unit cells are $(\pi/2-\delta)$ and $(2\pi/3-\delta)$, respectively.

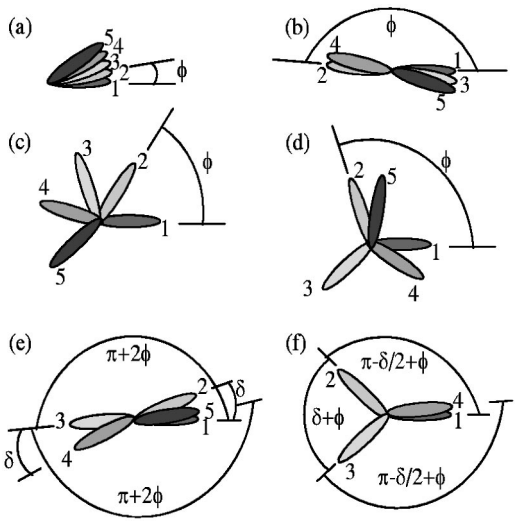

FIG. 2. (a)–(f) Cartoons depicting the tilt orientation of Sm C^*, Sm C_A^*, Sm $C_{\alpha 1}^*$, Sm $C_{\alpha 2}^*$, Sm C_{d4}^*, and Sm C_{d3}^*, respectively.

To summarize these phases, there are four simple helical phases, Sm C^*, Sm C_A^*, Sm $C_{\alpha 1}^*$, and Sm $C_{\alpha 2}^*$, each with a characteristic range of values for rotation of the c director from layer to layer. There are two distorted-helix phases, Sm C_{d4}^* and Sm C_{d3}^*, which possess an approximately four- and three-layer unit cell, respectively.

The molecular arrangements in the Sm-C_{d4}^* (Sm-C_{d3}^*) phase can be thought of as a simple distorted helix with pitch of about four layers (three layers). The distortion arises because $|\alpha_j - \alpha_{j+1}| \approx \pi/2$ costs energy, and distorting the helix can minimize G. In the Sm-C_{d4}^* phase, $|\delta|$ is greater than approximately $|\arcsin[-f_1/(2b\theta^2)]|$, where $|\delta|=\pi/2$ yields an undistorted helix. In the Sm-C_{d3}^* phase, no simple relation for δ was found.

Figure 3 exhibits the phase diagram for the parameters $a_3=-0.07$ K, $b\theta^2=-0.2$ K, and $f_1=0.12$ K as a function of a_1 and a_2. The parameters a_4, f_2, and f_3 should be smaller than the other coefficients and are thus set to zero for simplicity. We have simulated the system with other reasonable choices for a_4, f_2, and f_3 and found that these higher-order terms do not significantly affect the phase diagram. All the lower-order terms that are set to nonzero values are necessary to produce a phase diagram with all of the Sm-C^* variant phases, as is described below. Although the parameters a_1, a_2, a_3, and f_1 appear to depend on each other from the analysis of Čepič and Žekš [13], they are actually independent. In Ref. [13] the seven coefficients [i.e., a_i and f_i in Eq. (1)] describing the effective interlayer interactions are functions of seven other parameters. Thus taking the condition with $a_4=f_2=f_3\approx 0$, we still have enough freedom to

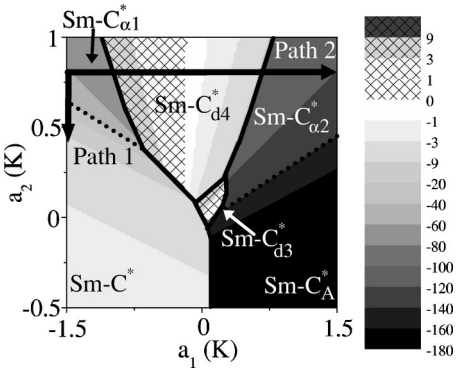

FIG. 3. Phase diagram plotted as a_2 versus a_1 for $a_3=-0.07$ K, $b\theta^2=-0.2$ K, $f_1=0.12$ K, and $a_4=f_2=f_3=0$. Path 1 and 2 are described in the text. The shades of gray represent ϕ.

set any value for the other four parameters: a_1, a_2, a_3, and f_1. So instead of assuming a specific form for the value of the various parameters, the simple approach of holding many values constant and letting others (a_1 and a_2) vary has been used. The values of the parameters held constant were chosen somewhat arbitrarily. The value of the ratio of $b\theta^2/f_1$ was chosen to give a distortion angle similar to that found in experiments [4,5]. Generally, the parameters may not be a simple function of temperature. The lines on the figure show phase boundaries, where dotted lines denote the transition from a simple helical solution to another in which the pitch appears to change smoothly. The shades of gray represent ϕ measured in degrees. The distortion angles are shown in Fig. 4, where the angle is defined to be zero in the simple helical phases.

From these figures we see that the Sm-C^* phase exists primarily in the region where a_1 and a_2 are negative, i.e., both favor $|\alpha_j-\alpha_{j+1}|\approx 0$. The Sm-$C^*_A$ phase is stabilized where $a_1>0$ and $a_2<0$. The Sm-C^*–Sm-C^*_A transition occurs at $a_1\approx -2a_3$. The Sm-C^*_{d4} phase is stable primarily where $a_2>0$ and a_1 is not too large; for the parameters chosen in the Sm-C^*_{d4} phase the distortion angle $\delta\approx 18°$. The Sm-C^*_α phase is stabilized in both the upper-left and upper-right regions of the figure where there is competition from the terms proportional to a_1 and a_2. The Sm-C^*_{d3} phase exists

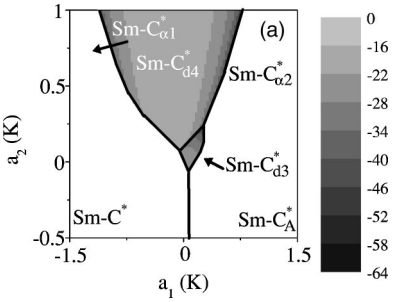

FIG. 4. (a) The distortion angle δ in degrees plotted as a_2 versus a_1 for $a_3=-0.07$ K, $b\theta^2=-0.2$ K, $f_1=0.12$ K, and $a_4=f_2=f_3=0$. The shades of gray represent δ. In the simple helical phases δ is taken to be zero.

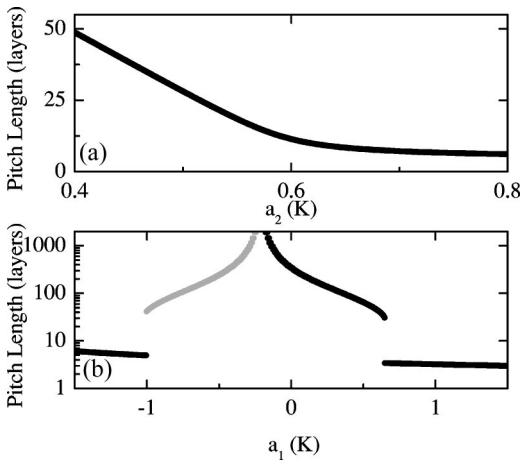

FIG. 5. (a) The pitch versus a_2 along path 1 for the Sm-$C^*_{\alpha 1}$–Sm-C^* transition. (b) The pitch versus a_1 along path 2 for the Sm-$C^*_{\alpha 1}$–Sm-C^*_{d4}–Sm-$C^*_{\alpha 2}$ transition.

only in a limited window near $a_1\approx a_2\approx 0$. For the parameters chosen, $\delta\approx 30°$ in the Sm-C^*_{d3} phase.

The values of the pitch have been plotted along the two paths indicated in Fig. 3. Figure 5(a) shows pitch versus a_2 (path 1) for $a_1=^-1.5$ K, thereby exhibiting the Sm-$C^*_{\alpha 1}$–Sm-C^* transition. As the transition is approached from Sm-$C^*_{\alpha 1}$, the pitch increases slowly, then grows quickly after the transition to Sm C^*. The pitch depicted in Fig. 5(b) follows path 2 with a_1 varying and $a_2=0.8$ K to show the Sm-$C^*_{\alpha 1}$–Sm-C^*_{d4}–Sm-$C^*_{\alpha 2}$ transition indicated by the jump in the pitch. The gray and black lines on the graph denote opposite handednesses of the pitch. For such a transition, the pitch decreases upon approaching Sm C^*_{d4} from Sm $C^*_{\alpha 1}$. After entering the Sm-C^*_{d4} phase the pitch becomes much larger and changes sign. Further along the path the pitch approaches infinity and changes sign again near $a_1\approx 3a_3$. The pitch becomes much smaller again after the Sm-C^*_{d4}–Sm-$C^*_{\alpha 2}$ transition and decreases further as a_1 increases. The change in pitch handedness in Sm C^*_{d4} is easy to understand if the phase is thought of as a distortion from a simple helix with a pitch length of ≈ 4 layers. If the pitch of the simple helix is less (greater) than 4, then the corresponding pitch in Sm C^*_{d4} has one (the opposite) handedness. The Sm-C^*_{d3} phase may also show the same feature, but we have not observed this in our calculation for reasonable parameter choices because of its limited stability window. Along path 2, δ does change. δ has a minimum when the pitch is longest, and increases near the Sm-$C^*_{\alpha 1}$–Sm-C^*_{d4} and Sm-$C^*_{\alpha 2}$–Sm-C^*_{d4} transitions.

The Sm-C^* phase has a left-handed helix for a negative ϕ. Measurements of the pitch in the Sm-C^*_A phase are typically of the two-layer unit cell, so that a negative ϕ leads to an right-handed helix in measurements. If f_1, f_2, and f_3 do not change greatly then ϕ should be of the same sign in both phases, and thus an opposite handedness of helical pitch will be measured in these two phases.

What are the essential criteria for the existence of the Sm-C^*_{d4} and Sm-C^*_{d3} phases? We find that for $b\theta^2<0$ the Sm-

C^*_{d4} phase exists. For Sm C^*_{d3}, it is also necessary to have a negative a_3.

In order to simplify the free-energy, it is useful to determine the minimum number of terms that are necessary to produce the complete phase sequence seen in experiments. For this only the terms proportional to a_1, a_2, a_3, f_1, and b and those having only to do with the mean-field expansion of $\vec{\xi}$ need to be considered. We have observed that the higher-order terms in the expansion do not significantly affect the phase sequence. So we may simplify Eq. (1) and write only the essential terms of the free-energy that should be the starting point for further theoretical work. This can be written as Eq. (2),

$$G = A\sum_{j=1}^{N}\left(\frac{T-T_0}{2}\vec{\xi}_j^2 + \frac{B}{4}\vec{\xi}_j^4 + f_1(\vec{\xi}_j\times\vec{\xi}_{j+1})_z + \sum_{i=1}^{3} a_i(\vec{\xi}_j\cdot\vec{\xi}_{j+i}) + b(\vec{\xi}_j\cdot\vec{\xi}_{j+1})^2\right). \quad (2)$$

The first two terms in Eq. (2) are the standard mean-field terms that describe a nonzero tilt below some critical temperature. The chiral term proportional to f_1 is necessary to describe the chiral properties of the Sm-C^* variant phases. The a_1 term is necessary to account for the Sm-C^* and Sm-C^*_A phases. While a term that favors antiparallel α in next-nearest-neighbor layers is needed to account for the Sm-C^*_{d4} phase. A term favoring parallel third-nearest-neighbor layers is required to stabilize the Sm-C^*_{d3} phase, and so the a_3 term is included. Finally, the term proportional to b is required to stabilize both the Sm-C^*_{d3} and Sm-C^*_{d4} phases by favoring tilt orientations that are nearly parallel or antiparallel in adjacent layers for negative b. No additional terms are necessary to describe the Sm-C^*_α phase.

An interesting question to explore is what happens when the other parameters vary? We have found that the topology of the phase diagram is relatively robust and does not change greatly as the parameters that were held constant in the examples given here are varied. As $b\theta^2$ approaches zero the phase space of the distorted-helix phases decreases. By increasing f_1, the helical pitch of the Sm-C^* and Sm-C^*_A phases becomes shorter. The sign of f_1 decides the handedness of the pitch. As the ratio between f_1 and $b\theta^2$ changes, so does δ in the distorted-helix phases. The larger $|b\theta^2|$ is relative to f_1, the more distorted the phases become. In the Sm C^*_{d4} the distortion angle is approximately equal to $|\arcsin[-f_1/(2b\theta^2)]|$ when the pitch length is large. a_3 does not have a large effect. It is most noticeable that as a_3 increases the Sm-C^*_{d3} phase becomes more stable.

Does Sm C^*_{d4} (Sm C^*_{d3}) describe Sm C^*_{FI2} (Sm C^*_{FI1})? The structures of Sm C^*_{d4} and Sm C^*_{d3} match what was proposed to explain the optical and resonant x-ray data [4,5]. Several experimentally measurable features could provide further evidence of the validity of this theory. The theory predicts that the Sm-C^*_{d4} pitch length passes through infinity and the pitch changes handedness for some phase space paths. Because different compounds travel through phase space differently as a function of temperature, some compounds should exhibit this feature. If the chirality terms do not change greatly, as they should not for most compounds, then the same handedness should be found for the Sm-C^*_{d3} pitch (assuming this is not one of the rare cases described below) and the measured Sm-C^*_A pitch, but the opposite for the Sm-C^* pitch. Although we can not rule out that the Sm-C^*_{d3} phase may exhibit the same pitch as Sm C^* in some compounds, we believe this will be quite rare as we could not produce this with reasonable choices of parameters.

The Sm-C^* variant phases are caused by the competition of polar and steric interactions which are of the same order of magnitude. Thus, small changes in temperature ($\sim$20 K) lead to a diverse group of phases. It is therefore expected that different compounds would have very different phase sequences as the interactions for these compounds should have different temperature dependencies. However, most of the compounds studied exhibiting these phases have the same basic molecular structure, so it is not surprising that the phase sequences is similar among these compounds (generally Sm C^*_α–Sm C^*–Sm C^*_{FI2}–Sm C^*_{FI1}–Sm C^*_A upon cooling). Compounds that differ in a critical manner may exhibit other phase sequences, such as Sm C^*_{FI2} observed at a higher temperature than Sm C^*.

This theory explains why three- and four-layer unit cells are stable for a range of parameters. Without the addition of a distortion there is no particular reason why a four-layer (three-layer) unit cell is favored over a helix with a pitch of length 4.5 layers (3.5 layers), for example. However, experiments demonstrate that the four-layer unit cell is stable in numerous compounds for a 1°–5° K temperature range [6]. The stability of these unit cells can be explained if they are distorted helical structures. Consider the Sm-C^*_{d4} phase with an infinite pitch length ($\phi=0$) when a_2 is positive. The next-nearest-neighbor interactions are at a minimum as the c directors of the next-nearest-neighbor layers are antiparallel. When a finite pitch ($\phi\neq 0$) appears, then there is a significant cost in the next-nearest-neighbor energy without a substantial gain in the nearest-neighbor energy. This implies that for a small change in the parameters, the state of the system will not change greatly, and thus the Sm-C^*_{d4} phase is stabilized. A similar argument follows for the Sm-C^*_{d3} phase.

Many compounds exhibit the Sm-$C^*_{\alpha 1}$ phase. Experimental results demonstrate that the variation of the pitch length through the Sm-$C^*_{\alpha 1}$–Sm-C^* transition shows either an abrupt jump from approximately five layers to several hundred layers [16] or a continuous evolution from 10 to 80 layers with a very fast change at the transition temperature [8]. Without a symmetry change through the Sm-$C^*_{\alpha 1}$–Sm-C^* transition this is similar to the liquid-gas transition. Thus the Sm-$C^*_{\alpha 1}$–Sm-C^* transition should have a first-order transition line that terminates at a critical point. Beyond the critical point, a continuous evolution between these two phases becomes possible. The Sm-$C^*_{\alpha 2}$ phase has just recently been experimentally identified by our research group in one compound [17].

IV. CONCLUSION

In summary, we have proposed a phenomenological free-energy containing what we believe is the minimum number of parameters necessary to describe the stability of all the observed Sm-C^* variant phases. In particular, this free-energy expansion with a proper set of parameters enable us to demonstrate the stability of the four- and three-layer unit cell with distorted helical structures. To the best of our knowledge this has not been previously achieved. We suggest that the distorted phases describe the Sm-C^*_{FI1} and Sm-C^*_{FI2} phases. The pitch length in the Sm-C^*_{FI2} phase is predicted to approach infinity and change signs along some paths through phase space (and thus for some compounds). The theory predicts a new distinct short helical pitch phase (Sm $C^*_{\alpha 2}$) with a pitch between two and four layers. During the review process of this manuscript our research group has successfully identified the existence of such a phase in one compound [17]. Further experimental characterization of the Sm-C^*_{FI2} and Sm-$C^*_{\alpha 2}$ phases of different liquid-crystal compounds are in progress to test this phenomenological model.

ACKNOWLEDGMENTS

This research was supported in part by the National Science Foundation, Solid State Chemistry Program, under Grant Nos. DMR-0106122 and 9901739.

[1] A. Chandani, E. Gorecka, Y. Ouchi, H. Takezoe, and A. Fukuda, Jpn. J. Appl. Phys., Part 2 **28**, L1265 (1989).
[2] M.A. Osipov and A. Fukuda, Phys. Rev. E **62**, 3724 (2000).
[3] T. Matsumoto, A. Fukuda, M. Johno, Y. Motoyama, T. Yui, S.-S. Seomun, and M. Yamashita, J. Mater. Chem. **9**, 2051 (1999).
[4] P.M. Johnson, D.A. Olson, S. Pankratz, T. Nguyen, J. Goodby, M. Hird, and C.C. Huang, Phys. Rev. Lett. **84**, 4870 (2000).
[5] A. Cady, J.A. Pitney, R. Pindak, L.S. Matkin, S.J. Watson, H.F. Gleeson, P. Cluzeau, P. Barois, A.-M. Levelut, W. Caliebe, J.W. Goodby, M. Hird, and C.C. Huang, Phys. Rev. E **64**, 050702 (2001).
[6] P. Mach, R. Pindak, A.-M. Levelut, P. Barois, H.T. Nguyen, C.C. Huang, and L. Furenlid, Phys. Rev. Lett. **81**, 1015 (1998).
[7] M. Škarabot, M. Čepič, B. Žekš, R. Blinc, G. Heppke, A.V. Kityk, and I. Muševič, Phys. Rev. E **58**, 575 (1998).
[8] A. Cady, D.A. Olson, X.F. Han, H.T. Nguyen, and C.C. Huang, Phys. Rev. E **65**, 030701 (2002).
[9] M. Yamashita and S. Miyazima, Ferroelectrics **48**, 1 (1993).
[10] A. Roy and N. Madhusudana, Europhys. Lett. **36**, 221 (1996).
[11] S. Pikin, M. Gorkunov, D. Kilian, and W. Haase, Liq. Cryst. **26**, 1107 (1999).
[12] R. Bruinsma and J. Prost, J. Phys. II **4**, 1209 (1994).
[13] M. Čepič and B. Žekš, Phys. Rev. Lett. **87**, 85501 (2001).
[14] M. Čepič and B. Žekš, Mol. Cryst. Liq. Cryst. Sci. Technol., Sect. A **301**, 221 (1997).
[15] B. Jin, Z. Ling, Y. Takanishi, K. Ishikawa, H. Takezoe, A. Fukuda, M.-A. Kakimoto, and T. Kitazume, Phys. Rev. E **53**, R4295 (1996).
[16] P. Mach, R. Pindak, A.-M. Levelut, P. Barois, H.T. Nguyen, H. Baltes, M. Hird, K. Toyne, A. Seed, J.W. Goodby, C.C. Huang, and L. Furenlid, Phys. Rev. E **60**, 6793 (1999).
[17] A. Cady, D.A. Olson, X.F. Han, H.T. Nguyen, H. Orihara, and C.C. Huang (unpublished).